Characterizing the Expression of CYP3A4 and Efflux Transporters (P-gp, MRP1, and MRP2) in CYP3A4-Transfected Caco-2 Cells After Induction with Sodium Butyrate and the Phorbol Ester 12-O-Tetradecanoylphorbol-13-Acetate

Carolyn L. Cummins,[1] Lara M. Mangravite,[1] and Leslie Z. Benet[1,2]

February 12, 2001; accepted April 27, 2001

Purpose. To examine the changes in expression levels of CYP3A4 and efflux transporters in CYP3A4-transfected Caco-2 (colon carcinoma) cells in the presence of the inducers sodium butyrate (NaB) and 12-O-tetradecanoylphorbol-13-acetate (TPA). To characterize the transport of [^{3}H]-digoxin and the metabolism of midazolam in the cells under different inducing conditions.

Methods. CYP3A4-Caco-2 cells were seeded onto cell culture inserts and were grown for 13–14 days. Transport and metabolism studies were performed on cells induced with NaB and/or TPA for 24 h. The expression and localization of P-gp, MRP1, MRP2, and CYP3A4 were examined by Western blot and confocal microscopy.

Results. In the presence of both inducers, CYP3A4 protein levels were increased 40-fold over uninduced cells, MRP2 expression was decreased by 90%, and P-gp and MRP1 expression were unchanged. Midazolam 1-OH formation exhibited a rank order correlation with increased CYP3A4 protein, whereas [^{3}H]-digoxin transport (a measure of P-gp activity) was unchanged with induction. P-gp and MRP2 were found on the apical membrane, whereas MRP1 was found perinuclear within the cell. CYP3A4 displayed a punctate pattern of expression consistent with endoplasmic reticulum localization and exhibited preferential polarization towards the apical side of the cell.

Conclusions. The present study characterized CYP3A4-Caco-2 cell monolayers when induced for 24 h in the presence of both NaB and TPA. These conditions provide intact cells with significant CYP3A4 and P-gp expression suitable for the concurrent study of transport and metabolism.

KEY WORDS: Caco-2 cells; CYP3A4; P-glycoprotein; MRP1; MRP2; confocal.

INTRODUCTION

The Caco-2 (colon carcinoma) cell line is currently used as the industry standard to model the human intestinal absorption of new compounds (1). Drug permeation rates across the cells have been shown to correlate well with the percent of drug absorbed in the body for passively absorbed, as well as actively transported compounds (2,3). Caco-2 cells express many absorptive transporters, including the bile acid, monocarboxylic acid, and dipeptide transporters (4). They also express several efflux transporters such as P-glycoprotein (P-gp) and the multidrug resistance associated transporters, MRP1 and MRP2 (5,6). However, Caco-2 cells fall short as a model for the intestine because they lack the most prevalent oxidative metabolizing enzyme found in the gut: cytochrome P450 3A4 (CYP3A4). Intestinal first-pass metabolism by CYP3A4 has been shown to be important in the disposition of several drugs, including midazolam and cyclosporine (7,8). Thus, a more physiologically accurate model of the human intestine would likely allow for better predictions of the oral absorption of drugs that are subject to intestinal first-pass metabolism.

Currently, there are two Caco-2 cell models that express CYP3A4 at high enough levels to allow the concurrent study of transport and metabolism. These systems include Caco-2 cells in which CYP3A4 expression is upregulated by adding 1α,25-dihydroxy vitamin-D_3 (di-OH vit D_3) to the growth medium (9), and the model discussed herein, Caco-2 cells transfected with CYP3A4 (10) (commercially available from Gentest, Woburn, MA). The di-OH vit D_3 cells are advantageous in that no external vector is introduced into the Caco-2 cells and the inducing agent is a naturally occurring hormone. Increases in other proteins such as P-gp and NADPH cytochrome P450 reductase were also observed in this system (9). A disadvantage in the use of the di-OH vit D_3-induced Caco-2 cells is their cost–they require an expensive inducing agent and laminin-coated inserts. In addition, the variability in the level of induction of CYP3A4 using di-OH vit D_3 has been reported to be as much as 4-fold between experiments (11).

In contrast, the CYP3A4-transfected Caco-2 cells (CYP3A4-Caco-2) are compatible with uncoated PET inserts as well as inexpensive inducing agents to increase CYP3A4 protein. Furthermore, the time to reach fully differentiated, tight, confluent monolayers is decreased from 21 to 14 days. The main drawback for the use of these cells is that the vector is progressively lost with increasing passage number [with a half-life of ~4 weeks (10)]. Therefore, to continue the use of the cell line at constant passage, a large stock at low passage number must be generated, although the addition of a DNA-methylation inhibitor to the cell growth medium has recently been shown to increase vector half-life (12). CYP3A4 expression and function in CYP3A4-Caco-2 cells can be increased significantly by pre-incubation with 12-O-tetradecanoylphorbol-13-acetate (TPA) or sodium butyrate (NaB) (10). The mechanisms of CYP3A4 induction in this cell line are not specifically known. However, TPA is a known inducer of protein kinase C, and NaB is capable of transcriptional activation through the inhibition of histone deacetylase. Due to the broad and non-specific nature of these inducers, one goal of this research was to explore the effects of these inducers on the expression of other proteins that are relevant to modulating intestinal drug absorption. Efflux transporters such as P-gp, MRP1, and MRP2 are known to be expressed in human intestine (13) and may play a role in the transport of xenobi-

[1] Department of Biopharmaceutical Sciences, University of California, San Francisco, California, 94143.

[2] To whom correspondence should be addressed. (e-mail: benet@itsa.ucsf.edu)

ABBREVIATIONS: P-gp, P-glycoprotein; MRP1, multidrug resistance-associated protein 1; MRP2, multidrug resistance-associated protein 2; CYP3A4, cytochrome P450 3A4; TPA, 12-O-tetradecanoylphorbol-13-acetate; NaB, sodium butyrate; di-OH vit D_3, 1α,25-dihydroxy vitamin-D_3; PET, polyethylene terephthalate; TEER, transepithelial electrical resistance; CLSM, confocal laser scanning microscopy; *ER*, extraction ratio.

0724-8741/01/0800-1102$19.50/0

otics. Characterizing the inducibility of the proteins involved in intestinal drug absorption will provide the opportunity to differentially modulate the levels of these proteins and study their interplay *in vitro*.

MATERIALS AND METHODS

Materials

CYP3A4-transfected Caco-2 cells were obtained from Gentest (Woburn, MA). Dulbecco's modified Eagle's medium containing 8.5 g/l glucose, 25 mM HEPES, and 2.2 g/l $NaHCO_3$ and nonessential amino acids (NEAA) was obtained (custom made) from the UCSF Cell Culture Facility (San Francisco, CA). Fetal bovine serum was obtained from HyClone Laboratories (Logan, UT) and Hygromycin B was purchased from Gibco-BRL (Gaithersburg, MD). Falcon PET cell culture inserts and Costar 6-well plates were obtained from Fisher Scientific (Santa Clara, CA). NaB and TPA were purchased from Sigma (St. Louis, MO). [^{14}C]-Mannitol (51 mCi/mmol) and [^{3}H]-digoxin (19 Ci/mmol) were purchased from NEN (Boston, MA). Midazolam and 1-OH midazolam were kindly provided by Hoffmann-LaRoche (Nutley, NJ). P-gp antibody C219 was obtained from Signet (Dedham, MA) and P-gp antibody MRK16 as well as MRP1 antibody (MRPr1) and MRP2 antibody (M_2III-6) were purchased from Kamiya Biomedical Company (Seattle, WA). CYP3A4 antibody (WB-3A4) was obtained from Gentest. FITC-conjugated ZO-1 antibody was obtained from Zymed Laboratories (San Francisco, CA). Texas-red conjugated-phalloidin was purchased from Molecular Probes (Eugene, OR). FITC-conjugated goat anti-mouse, FITC-conjugated goat anti-rat, and Cy5-conjugated goat anti-mouse were purchased from Gibco-BRL, Sigma, and Chemicon International (Temecula, CA), respectively.

Cell Culture Growth Conditions

CYP3A4-Caco-2 cells (passages 4 and 5) were seeded at a density of 300,000 cells/insert and were grown to confluence for 13 to 14 days. Twenty-four hours prior to an experiment, the cell culture media was replaced with growth media containing either 4 mM NaB and/or 100 nM TPA for protein induction.

Assessing Cell Monolayer Integrity

Transepithelial electrical resistance (TEER) was measured across the monolayer using the Millipore Millicell (Bedford, MA) equipped with chopstick electrodes. The resistance (in ohms) was measured across the monolayer when the cells were incubating in transport buffer (Hanks' BSS with 25 mM HEPES, pH 7.4) at 37°C. Background resistances were obtained from empty inserts. The TEER values were calculated as the background subtracted resistance multiplied by the surface area of the insert (4.2 cm^2).

Transport Studies and Midazolam Metabolism in Cell Monolayers

Cell monolayers were pre-incubated in transport buffer for 30 min at 37°C. The study was initiated by adding the test compound (1.96 μM [^{14}C]-mannitol, 30 nM [^{3}H]-digoxin, or 3 μM midazolam) to the donor compartment and transport buffer to the receiver compartment. The final volume in each of the chambers was 1.5 ml on the apical side and 2.5 ml on the basolateral side. For radiolabeled compounds, 100-μl samples were obtained at 1 h (for mannitol) or at 0.5, 1, and 2 h (for digoxin) and added to scintillation vials. Five milliliters of scintillation cocktail (Econo-Safe, RPI, Mount Prospect, IL) was added and samples were counted in a Beckman LS180 counter (Beckman Instruments, Palo Alto, CA). For the midazolam studies, 500-μl samples were obtained after 30 min from the apical and basolateral chambers. Intracellular measurements of midazolam and 1-OH midazolam were obtained by solubilizing the cell culture inserts with 1 ml of 70:30 MeOH:H_2O and sonicating on ice. The homogenate was centrifuged for 5 min at 10,000 × g and the resulting supernatant was analyzed by LC-MS.

Cell Lysis and Western Blotting

Cells were harvested from six cell culture inserts and collected in ice-cold PBS (Ca^{+2} and Mg^{+2} free). The sample was washed twice with PBS, resuspended in lysis buffer (10 mM Tris-HCl, 10 mM KCl, and 1.5 mM $MgCl_2$, pH 7.4, with protease inhibitors: 2 μg/ml leupeptin, 1 μg/ml pepstatin, 2 μg/ml aprotinin, and 1 mM PMSF), sonicated on ice, and stored at −80°C until analysis. Protein concentrations were measured using the Bio-Rad protein assay (Hercules, CA) with BSA as a standard. Samples were electrophoresed on 4%–20% gradient gels (Bio-Rad) and transferred to nitrocellulose using standard techniques. The blot was blocked in 3% non-fat milk and incubated with primary antibody: C219 (1:500 dilution), MRPr1 (1:50), M_2III-6 (1:50), or WB-3A4 (1:3,000), washed with TTBS (Tris-buffered saline containing 0.05% Tween-20), and incubated with secondary HRP-conjugated antibody, goat anti-mouse for P-gp, MRP2, and CYP3A4 or goat anti-rat for MRP1 (1:3,000). The signal was observed using ECL detection (Amersham) and was quantified using a Pharmacia LKB Ultroscan XL densitometer (Pharmacia, Alameda, CA). Each Western blot was repeated a minimum of two times per sample set (two plates per induction condition = 1 sample set) with a total of three sample sets obtained.

Confocal Microscopy

Confluent cells cultured on inserts were fixed with 4% paraformaldehyde, permeabilized using 0.025% saponin, blocked using 10% horse serum, and stained for indirect immunofluorescence with primary antibodies MRPr1, M_2III-6, and MRK16 (1:4 dilution) or WB-3A4 (1:100 dilution). Secondary antibodies (FITC- or Cy5- conjugated goat anti-mouse 1:500 for MRP2, CYP3A4, and P-gp, and FITC-conjugated goat anti-rat 1:320 for MRP1) were incubated in the presence of either a plasma membrane stain for actin (Texas Red-X phalloidin, 1:40 dilution) or a tight junction marker (FITC-labeled zonula occludens antibody, 1:100 dilution). Filters were mounted in Vectashield (Vector Laboratories, Burlingame, CA) and visualized using a Bio-Rad MRC-1024 confocal laser scanning microscope.

Data Analysis

Calculation of the extraction ratio of midazolam was performed employing a variation of the equation used by Fisher

Table I. Effects of Inducers NaB and TPA on CYP3A4-Caco-2 Cell Monolayer Integrity[a]

	Induction Condition			
	No induction	4 mM NaB	100 nM TPA	NaB and TPA
TEER (ohm · cm^2)	796 ± 34	582 ± 50[b]	557 ± 42[b]	330 ± 63[b]
[^{14}C]-Mannitol $P_{app} \times 10^6$ (cm/s)	1.35 ± 0.07	1.08 ± 0.06	1.29 ± 0.02	3.7 ± 0.9[b]

[a] Data are presented as means ± SD ($n = 6$).
[b] Statistically different from no induction control ($p < 0.05$).

et al. (14). The present equation incorporates in the denominator the intracellular levels of unchanged midazolam, as it is reasoned that if the drug is inside the cell, it could interact with CYP3A4.

$$ER = \frac{\sum 1\text{-OH midazolam}_{(\text{all chambers})}}{\sum \text{midazolam}_{(\text{receiver, intracellular})} + \sum 1\text{-OH midazolam}_{(\text{all chambers})}} \quad (1)$$

The permeability values were calculated using the following equation:

$$P_{app} = \frac{\text{rate of transport}}{\text{surface area} \times \text{donor concentration}} \quad (2)$$

One-way ANOVA followed by the Tukey test was used to determine significance of data. The prior level of significance was set at $p < 0.05$.

RESULTS

Effects of Inducers on Monolayer Integrity

Cells grown for 24 h in the presence of 4 mM NaB, 100 nM TPA, or both NaB and TPA were found to have lower TEER values than their uninduced counterparts (Table I). When the inducers were dosed individually, a 30% decrease from the control TEER value was observed, whereas with both inducers together, a decrease of 60% from the uninduced cells was obtained. The transport of the paracellular marker mannitol was used to study the integrity of the tight junctions between cells in the presence of the inducers. [^{14}C]-Mannitol transport was not adversely affected by the presence of NaB or TPA alone, however, a 2.7-fold increase in mannitol P_{app} was observed for the cells induced with both NaB and TPA (Table I).

Western Blotting of Efflux Transporters

The inducers NaB and TPA were found to have differential effects on the expression of the transporters P-gp, MRP1, and MRP2 (Fig. 1). The protein band intensities were quantitated by densitometry (Table II). P-gp protein expression consistently appeared to be increased in the presence of NaB, but no increase in P-gp was observed in the presence of TPA. However, due to the variability in the band intensities, the apparent increase with NaB did not reach statistical significance. The MRP1 protein levels were unaltered in the presence of NaB or TPA (alone or in combination), whereas MRP2 protein levels were significantly decreased. MRP2 levels were reduced to one-third of the control value when cells were grown in the presence of either NaB or TPA alone and decreased further (to 10% of control) with both inducers ($p < 0.05$).

P-gp Transporter Activity

The transport of the P-gp substrate digoxin was tested across monolayers under all inducing conditions to determine if increased P-gp expression observed with NaB correlated with changes in P-gp activity. The net transport across the monolayer in the (B)asolateral to (A)pical direction exceeded that in the A to B direction, indicating that P-gp was functional in this cell line. Figure 2 shows the results of digoxin transport across CYP3A4-Caco-2 cells that have been induced with NaB, TPA, or both compounds. The calculated P_{app} values indicate that there was no change in the efflux activity of P-gp when pre-incubated with NaB (control vs. NaB $P_{app\ (B\ to\ A)}$: 5.26 ± 0.04 vs. 5.48 ± 0.17 × 10^{-6} cm/s), the treatment tending towards the greatest densitometric increase from Western blot.

Confocal Laser Scanning Microscopy (CLSM)

The localization of CYP3A4 and the efflux transporters P-gp, MRP1, and MRP2 in CYP3A4-Caco-2 cells was investigated by indirect immunofluorescence using CLSM. P-gp was localized to the apical membrane (Fig. 3A), consistent with previous studies in untransfected Caco-2 cells (15,16). MRP1, however, was found intracellular and peri-nuclear with no apparent plasma membrane staining (Fig. 3B). This finding is in contrast to the localization of MRP1 in LLCPK1-MRP1 expressing cells in which MRP1 was primarily on the lateral membranes with limited intracellular staining (17). The membrane location of MRP2 in CYP3A4-Caco-2 cells

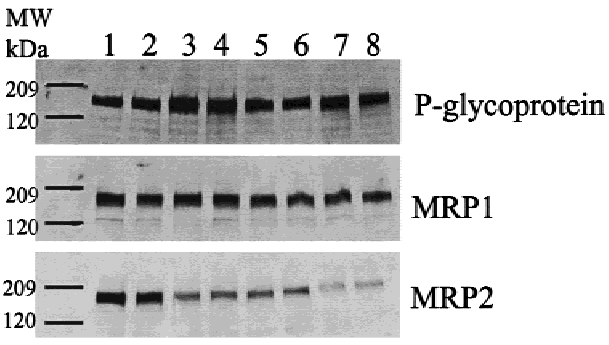

Fig. 1. Western blot of CYP3A4-Caco-2 cell homogenates probed for the efflux transporters P-gp, MRP1, and MRP2. The cells were grown in growth medium (control: lanes 1 and 2) or in the presence of the inducers 4 mM NaB (lanes 3 and 4), 100 nM TPA (lanes 5 and 6), or both NaB and TPA (lanes 7 and 8) for 24 h prior to the experiment. Each lane contains 12.5 μg of cell lysate.

Table II. Quantitative Comparison of Induction Conditions on Protein Levels of Efflux Transporters and CYP3A4 Using Densitometry[a]

	Induction Condition			
	No induction	4 mM NaB	100 nM TPA	NaB and TPA
P-glycoprotein	1.0 ± 0.4[b]	1.9 ± 0.4	0.9 ± 0.1	1.4 ± 0.1
MRP1	1.0 ± 0.3	0.9 ± 0.1	0.7 ± 0.1	0.8 ± 0.1
MRP2	1.0 ± 0.3	0.31 ± 0.05[c]	0.26 ± 0.01[c]	0.10 ± 0.01[c]
CYP3A4	1.0 ± 0.1	10.5 ± 0.7[c]	5.4 ± 0.5[c]	41 ± 1[c]

[a] Control cells were normalized to 1.0.
[b] Data are presented as the means ± SD of $n = 2$ samples.
[c] Statistically different from no induction control ($p < 0.05$).

was apical (Fig. 3C), in agreement with studies performed in MRP2-transfected MDCK cells (18). The localization of P-gp, MRP1, MRP2, and CYP3A4 was unchanged regardless of the inducing condition, although a marked decrease in the intensity of MRP2 staining and a significant increase in the CYP3A4 staining was observed in the NaB- and TPA-induced cells (consistent with the Western blot results). The actin-staining pattern, however, was more diffuse when cells were induced with both NaB and TPA. The images in Fig. 3, A, B, and C were, therefore, obtained from uninduced cells where the actin was more closely associated with the plasma membrane.

CYP3A4 was localized around the nucleus in a punctate pattern consistent with a location on the endoplasmic reticulum (Fig. 3D). These cells were costained with a protein closely associated with tight junctions, zonula occludens 1 (ZO-1), which delineates the barrier between the apical and basolateral membranes. The vertical cross-section of the sample revealed increased staining of CYP3A4 near the apical side of the cell. This was confirmed by optically sectioning the sample in the x-y plane at regularly spaced distances along the z-axis starting at the apical membrane (Fig. 4). Negative controls were performed to determine the extent of nonspecific binding for each sample using cells incubated with only the secondary antibody. For all antibodies studied, either no staining or only very weak and diffuse staining for the negative controls was observed.

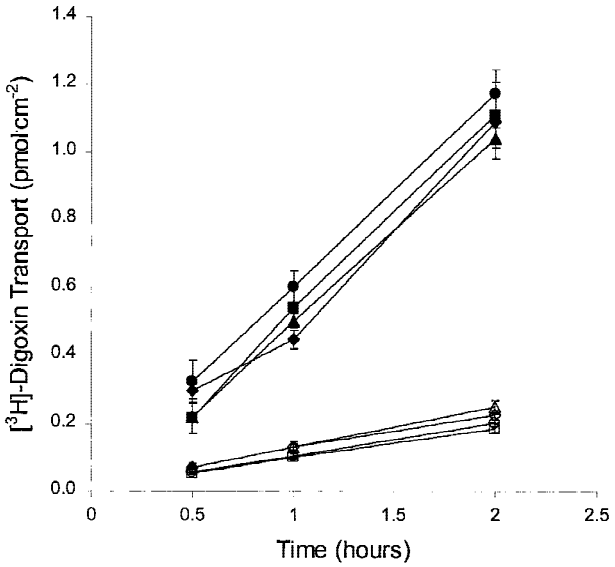

Fig. 2. Transepithelial flux of digoxin across CYP3A4-Caco-2 cells. Digoxin fluxes in the B→A direction are plotted with solid symbols and fluxes in the A→B direction are indicated by open symbols. Control cells (•) or cells pretreated with NaB (■), TPA (♦), or both NaB and TPA (▲) were found to have similar bidirectional transport characteristics. Concentration of digoxin was 30 nM. Data are illustrated as the means ± SD ($n = 3$).

CYP3A4 Activity and Expression with Inducers

CYP3A4 protein levels were significantly increased when cells were incubated with the inducers alone or in combination as measured by Western blot (Fig. 5A). The increase obtained with both NaB and TPA was 40-fold over the control levels and was greater than that obtained with either inducer alone (NaB and TPA, 10-fold and 5-fold, respectively; Table II). The CYP3A4 activity was measured by studying the metabolism of midazolam (a CYP3A4 marker compound) across the monolayer. The total sum of 1-OH midazolam metabolites formed after incubating 3 μM midazolam for 30 min was calculated for cells pre-incubated with or without inducers (Fig. 5B). There was a 40-fold increase in metabolism when cells were pretreated with both NaB and TPA compared to uninduced cells, consistent with the Western blot results. However, there was only a 3- and 2-fold increase in metabolism when cells were pre-incubated with NaB or TPA, respectively. The differential activity of CYP3A4 with the inducers showed a rank order correlation with the data obtained from Western blot. The high rate of metabolism in cells induced with both NaB and TPA resulted in a decreased amount of midazolam inside and across the cell monolayer (Fig. 5C).

Distribution of 1-OH Midazolam and Midazolam Extraction Ratio

Table III shows the distribution of 1-OH midazolam across the cell monolayer at 30 min. Under all the inducing conditions, there was preferential sorting of 1-OH midazolam to the apical membrane. This data is in agreement with the preferential apical sorting of 1-OH midazolam observed across di-OH vit D_3-induced Caco-2 cells (9,14). A midazolam extraction ratio was calculated based on these results using equation 1 and are shown in Table III. The extraction ratios varied between 0.9% to 32% for control cells versus cells induced with both NaB and TPA.

DISCUSSION

Cytochrome P450 3A4 is the most abundant P450 in the human intestine (19) and has been reported to play an im-

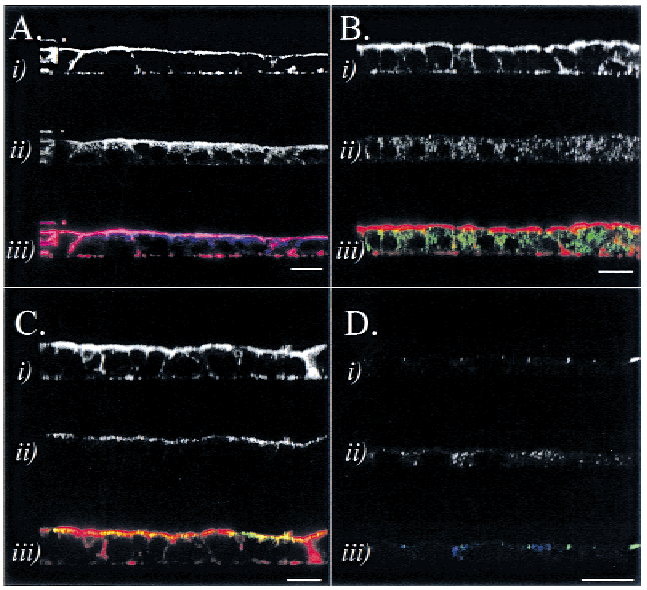

Fig. 3. Confocal microscopy of CYP3A4-Caco-2 cells examining the localization of P-gp (A.*ii*)), MRP1 (B.*ii*)), MRP2 (C.*ii*)), and CYP3A4 (D.*ii*)) by indirect immunofluorescence. Vertical optical sections are shown with the apical membrane on top. Each sample was co-stained for either actin (A.*i*), B.*i*), C.*i*)), or the tight-junction marker ZO-1 (D.*i*)). Individual fluorescence channels were probed independently (parts *i* and *ii*) and then together to obtain a merged image (part *iii*). In the merged images actin appears red (A, B, and C) and ZO-1 is green (D). P-gp (A.*iii*)) and CYP3A4 (D.*iii*)) were probed with Cy-5-conjugated secondary antibody (blue), whereas MRP1 (B.*iii*)) and MRP2 (C.*iii*)) were probed with FITC-conjugated secondary antibody (green). When co-localized, blue and red appear pink (A.*iii*) (apical side) and green and red appear yellow (C.*iii*) (apical side). Images A, B, and C were obtained from uninduced cells, whereas image D was from cells pre-treated with both NaB and TPA. Bars = 30 μm.

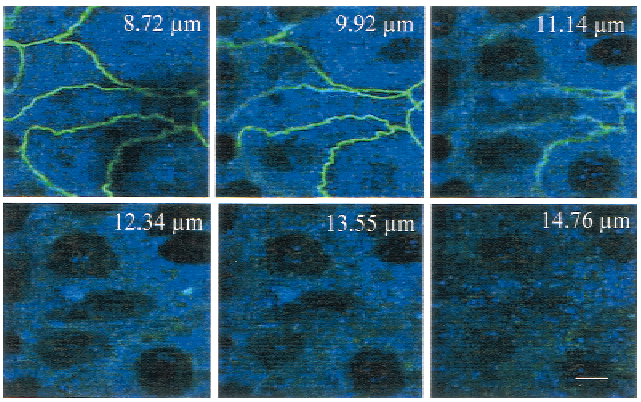

Fig. 4. Optical sections of the CYP3A4-Caco-2 cells obtained in the x-y plane using CLSM. Cells stained for CYP3A4 (blue) and ZO-1 (green) were progressively sectioned at 1.2-μm intervals. The position of each image is reported (relative to an arbitrary starting value) in the figure. The top three panels represent the three sections closest to the apical membrane (top left) where ZO-1 staining is visible. The CYP3A4 staining intensity was greatly decreased as the sections progressed towards the basolateral membrane (bottom right). Bar = 10 μm.

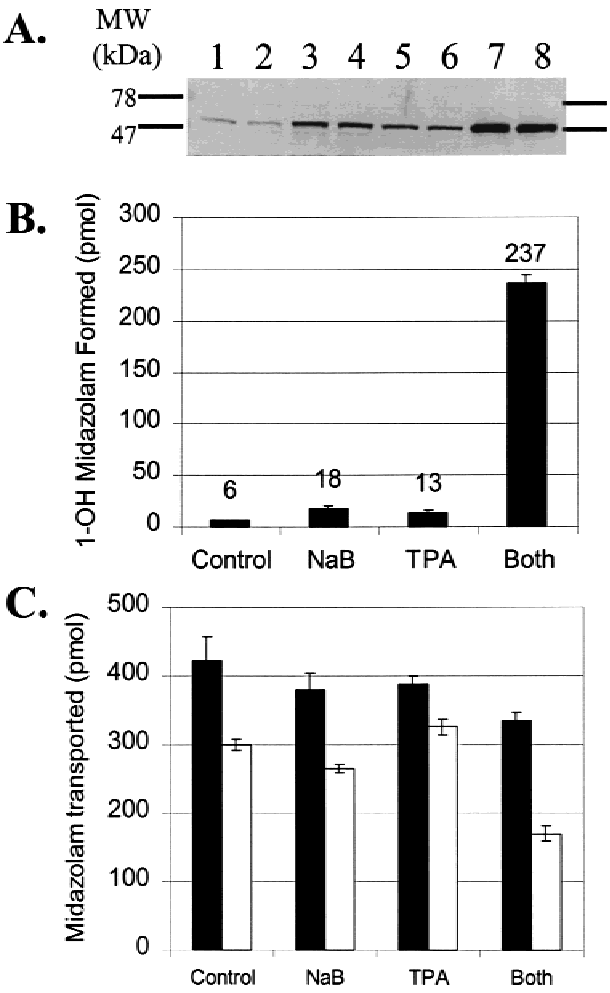

Fig. 5. Effect of the inducers NaB and TPA on the expression and function of CYP3A4 protein in CYP3A4-Caco-2 cells. (A) Western blot of CYP3A4 protein from CYP3A4-Caco-2 cell homogenates (12.5 μg loaded). The cells were grown in growth medium (control: lanes 1 and 2), or in the presence of the inducers 4 mM NaB (lanes 3 and 4), 100 nM TPA (lanes 5 and 6), or both NaB and TPA (lanes 7 and 8) for 24 h prior to the experiment. (B) CYP3A4 activity measured by formation of 1-OH midazolam after 30 min of incubation with apically dosed 3 μM midazolam ($n = 3$). (C) Effect of increased expression of CYP3A4 on the transcellular transport of midazolam across the cell monolayer. After 30 min, the amount of midazolam found on the basolateral side (solid bars) and the amount of intracellular midazolam (open bars) was measured. Data in B and C are represented as means ± SD ($n = 3$).

portant role in drug metabolism (20). Its location in the intestinal columnar epithelial cells allows it to come into direct contact with drugs that are transcellularly absorbed along the intestinal tract. The addition of extrachromosomal CYP3A4 to Caco-2 cells provides an intact cell model in which to study metabolic processes *in vitro*. Furthermore, the endogenous expression of efflux transporters such as P-gp, MRP1, and MRP2 in Caco-2 cells make it an appropriate model to study intestinal absorption. The present study investigated the inducing conditions under which the CYP3A4-Caco-2 cells should be grown to be ideally suited for the concurrent study of transport and metabolism.

Crespi *et al.* (10) showed CYP3A4-Caco-2 cells differen-

Table III. Distribution of 1-OH Midazolam[a] Across CYP3A4-Caco-2 Cells[b]

CYP3A4-Caco-2 cells induced with:	1-OH MDZ formed (pmol)			1-OH MDZ formation rate (pmol/min)	Basolateral MDZ (% apical dose)	Intracellular MDZ (% apical dose)	Extraction ratio (%)
	Apical	Basolateral	Intracellular				
No Induction	5.2 ± 0.7	bld[d]	1.2 ± 0.3	0.21 ± 0.02	9.4 ± 0.8	6.7 ± 0.2	0.9 ± 0.1
4 mM NaB	13 ± 3	bld	5.0 ± 0.5	0.60 ± 0.10[c]	8.5 ± 0.5	5.9 ± 0.1[c]	2.7 ± 0.4[c]
100 nM TPA	11 ± 3	bld	2.4 ± 0.6	0.44 ± 0.09	8.6 ± 0.3	7.2 ± 0.3	1.8 ± 0.4
NaB and TPA	158 ± 7[c]	22.8 ± 0.6	56 ± 3[c]	7.9 ± 0.2[c]	7.4 ± 0.3[c]	3.8 ± 0.3[c]	32 ± 1[c]

[a] Midazolam (3 μM) was applied to the apical chamber and was incubated for 30 min at 37°C.
[b] Data is presented as the means ± SD ($n = 3$).
[c] Statistically different from no induction control ($p < 0.05$).
[d] bld, below the limit of detection.

tiate and form tight, confluent monolayers after 13 days in culture. It was reported that TPA pretreatment resulted in increased CYP3A4 expression without loss of monolayer integrity, whereas NaB increased expression but caused the cells to be leaky. In contrast, our results indicate that the increased expression of CYP3A4 with NaB or TPA alone does not come at the expense of monolayer integrity, but instead it is the combination of NaB and TPA that causes the increased paracellular permeability. However, the mannitol P_{app} obtained from cells induced with both NaB and TPA (3.7×10^{-6} cm/s) was still found to be close to the range of reported literature values for Caco-2 cells ($0.65–3.2 \times 10^{-6}$ cm/s) (3,16,21). Furthermore, it has often been stated that Caco-2 cells have tight junctions that are tighter than the intestinal epithelium that they are modeling (22). Therefore, although the induction conditions increase paracellular permeability, it may result in generating a better *in vitro* model for intestinal absorption.

P-gp is a drug efflux pump present on the apical surface of human intestinal epithelial cells and is thought to be important in limiting the absorption of many drugs currently on the market. The bulk of P-gp in the CYP3A4-Caco-2 cells was found on the apical membrane by confocal microscopy, with a weaker P-gp signal just below the apical membrane as well as on the lateral membranes. Modest modulation of the P-gp protein levels was achieved with pre-incubation of the cells with NaB, but there was no corresponding increase in P-gp activity as investigated by the transport of digoxin. This may be an indication that the induction time was too short for the upregulated protein to be inserted into the membrane.

The multidrug resistance associated transporters MRP1 and MRP2 are two members of a large family of transporter proteins that have been reported to be expressed in the human intestine (13) and are capable of mediating ATP-dependent efflux of anionic drugs and drug- (glutathione, glucuronide, and sulfate) conjugates (18). Reports of MRP1 protein expression and localization in intestinal cells have been inconsistent. In Caco-2 cells, two research groups (5,23) have reported the expression of MRP1 by Western blotting using the MRPr1 antibody. However, other groups have reported little MRP1 expression in Caco-2 cells by Northern blot (6) and no expression by either Western blot (24) or confocal microscopy (25).

In CYP3A4-Caco-2 cells we observed significant expression of MRP1 by both Western blot and confocal microscopy using the MRPr1 antibody (which does not cross react with MRP2, MRP3, or MRP5 [26]). The peri-nuclear location of MRP1 within the CYP3A4-Caco-2 cells was consistent with its localization in normal human intestinal epithelial cells where it was found in the apical cytoplasmic region with no brush border staining (27), but contrasts the basolateral membrane location observed in LLC-PK1 MRP1-transfected cells (17) and the membrane staining seen in many tumor cell lines (28). The discrepancies in the expression of MRP1 in Caco-2 cells between laboratories could be due to differences in cell culture conditions (which have been shown to affect P-gp expression [16]) or cell passage number, as increasing Caco-2 passage number results in decreased MRP1 expression (23). The apical localization of MRP2 in CYP3A4-Caco-2 cells is consistent with its location in untransfected Caco-2 cells (25) and in rat (29) and rabbit (30) intestinal epithelia. The decreased expression of MRP2 in the CYP3A4-Caco-2 cells induced with NaB and TPA is the first report of such modulation of MRP2 and will require further investigation to identify the mechanism by which this decrease occurs.

It was previously unknown whether the increase in CYP3A4 protein obtained after induction was from upregulation of the endogenous CYP3A4 DNA or from the transfected CYP3A4 gene. Western blots performed on homogenates of untransfected Caco-2 cells (from our laboratory) that had been induced with NaB and TPA alone or in combination revealed no changes in the CYP3A4 level. In fact, no CYP3A4 protein was visible in the untransfected Caco-2 cells under any of the growth conditions (data not shown), suggesting that the observed changes in CYP3A4 levels in CYP3A4-Caco-2 cells were most likely due to the inducers acting on the extrachromosomal vector within the cells.

Using confocal microscopy, CYP3A4 was localized around the nucleus, consistent with its known location on the endoplasmic reticulum. The spatial location of CYP3A4 inside the cell appeared more apical than basolateral. This polarization of CYP3A4 within the cell is consistent with the staining observed in human intestine where the enzyme was preferentially located near the apical membrane in the columnar epithelial cells (19). The 40-fold increase in protein expression of CYP3A4 obtained after pre-incubating the CYP3A4-Caco-2 cells with NaB and TPA also translated into a 40-fold increase in CYP3A4 enzyme activity as measured by the rate of 1-OH midazolam formation. Sink conditions were maintained for all inducing conditions, as less than 10% of the donor had crossed to the receiver. When cells were induced with both NaB and TPA, significant metabolism resulted in

decreased transcellular transport across the membrane as well as decreased intracellular midazolam. This is evidence that the rate of metabolism in this cell line was sufficient to alter the net flux across the cell.

The midazolam incubation conditions (3 μM apical dose for 30 min) were chosen so that the metabolism results obtained from the CYP3A4-Caco-2 cell system could be compared with those obtained by Fisher *et al.* (14) using the di-OH vit D_3-induced Caco-2 cell system. When the 1-OH midazolam formation rate was compared between systems, it was found that CYP3A4-Caco-2 cells had a 2.5-fold greater rate of metabolism (7.9 pmol/min) compared with the di-OH vit D_3 system (2.99 pmol/min) (14). As a result, the extraction ratio from the CYP3A4-Caco-2 cells was 42% ± 3% (when calculated using the method of Fisher), while the extraction ratio obtained using the di-OH vit D_3 cells(14) was 14.5% ± 3.1 %. In contrast to Fisher's calculation, our CYP3A4-Caco-2 *ER* (calculated using equation 1) was 32% ± 1%. We did not consider the formation of 4-OH midazolam in our equation, as it was found to be minimal at this low dose of midazolam. In addition, we included in the denominator of equation 1 the amount of intracellular midazolam at 30 min, reasoning that if it was inside the cell it could interact with CYP3A4. However, both of these differences in the *ER* calculation caused our *ER* to be lower than that calculated using the method of Fisher *et al.* (14) since the intracellular midazolam accounted for 3.8% of the apical dose (Table III). Therefore, we conclude that at least for midazolam, the CYP3A4-Caco-2 cells induced with both NaB and TPA correlated reasonably well with the first pass extraction of midazolam across the human intestine calculated from an *in vivo* study performed in liver transplant patients ($ER = 43 \pm 18$) (7). However, caution should be exercised when interpreting *ER* results from *in vitro* data, as the values obtained will vary depending on the concentration of substrate and the time at which the *ER* is measured.

In conclusion, we have demonstrated that induction of CYP3A4-Caco-2 cells for 24 h with 4 mM NaB and 100 nM TPA provides a practical system in which to perform *in vitro* transport and metabolism studies. The induced cells express high levels of CYP3A4, permitting easier detection of metabolites while retaining the apical expression and efflux properties of P-gp. The close proximity of CYP3A4 to the brush border membrane where P-gp is located (as in human intestinal epithelia) supports the use of these cells as an *in vitro* model to study the interplay between these proteins occurring in the intestine. CYP3A4-Caco-2 cells, when induced, may be especially useful for predicting intestinal permeation rates and first pass intestinal metabolism, as well as providing a more realistic model in which to study intestinal drug-drug interactions.

ACKNOWLEDGMENTS

We gratefully acknowledge the financial support provided in part by the National Institutes of Health (grant no. CA72006 to L.Z.B.), by the National Institutes of Health Pharmaceutical Chemistry, Pharmacology and Toxicology Training Grant (no. GM07175 L. M. M.), and by the Affymax Research Institute (to C.L.C.). We thank Dr. Laurent Salphati for his helpful comments and suggestions. Dr. Benet has a financial interest in and serves as Chairman of the Board of AvMax, Inc., a biotechnology company whose main interest is in increasing drug bioavailability by inhibiting intestinal CYP3A and P-glycoprotein.

REFERENCES

1. P. Artursson and R. T. Borchardt. Intestinal drug absorption and metabolism in cell cultures: Caco-2 and beyond. *Pharm. Res.* **14**: 1655–1658 (1997).
2. P. Artursson and J. Karlsson. Correlation between oral drug absorption in humans and apparent drug permeability coefficients in human intestinal epithelial (caco-2) cells. *Biochem. Biophys. Res. Commun.* **175**:880–885 (1991).
3. S. Yee. *In vitro* permeability across caco-2 cells (colonic) can predict *in vivo* (small intestinal) absorption in man: Fact or myth. *Pharm. Res.* **14**:763–766 (1997).
4. A. Tsuji and I. Tamai. Carrier-meditated intestinal transport of drugs. *Pharm. Res.* **13**:963–977 (1996).
5. H. Gutmann, G. Fricker, M. Török, S. Michael, C. Beglinger, and J. Drewe. Evidence for different ABC-transporters in caco-2 cells modulating drug uptake. *Pharm. Res.* **16**:402–407 (1999).
6. T. Hirohashi, H. Suzuki, X.-Y. Chu, I. Tamai, A. Tsuji, and Y. Sugiyama. Function and expression of multidrug resistance-associated protein family in human colon adenocarcinoma cells (caco-2). *J. Pharmacol. Exp. Ther.* **292**:265–270 (2000).
7. M. F. Paine, D. D. Shen, K. L. Kunze, J. D. Perkins, C. L. Marsh, J. P. McVicar, D. M. Barr, B. S. Gillies, and K. E. Thummel. First-pass metabolism of midazolam by the human intestine. *Clin. Pharmacol. Ther.* **60**:14–24 (1996).
8. C.-Y. Wu, L. Z. Benet, M. F. Hebert, S. K. Gupta, M. Rowland, D. Y. Gomez, and V. J. Wacher. Differentiation of absorption and first-pass gut and hepatic metabolism in humans: Studies with cyclosporine. *Clin. Pharmacol. Ther.* **58**:492–497 (1995).
9. P. Schmiedlin-Ren, K. E. Thummel, J. M. Fisher, M. F. Paine, K. S. Lown, and P. B. Watkins. Expression of enzymatically active CYP3A4 by caco-2 cells grown on extracellular matrix-coated permeable supports in the presence of 1α,25-dihydroxy-vitamin-D_3. *Mol. Pharmacol.* **51**:741–754 (1997).
10. C. L. Crespi, B. W. Penman, and M. Hu. Development of caco-2 cells expressing high levels of cDNA-derived cytochrome P4503A4. *Pharm. Res.* **13**:1635–1641 (1996).
11. J. H. Hochman, M. Chiba, J. Nishime, M. Yamazaki, and J. H. Lin. Influence of p-glycoprotein on the transport and metabolism of indinavir in caco-2 cells expressing cytochrome P-450 3A4. *J. Pharmacol. Exp. Ther.* **292**:310–318 (2000).
12. M. Hu, Y. Li, C. M. Davitt, S.-M. Huang, K. E. Thummel, B. W. Penman, and C. L. Crespi. Transport and metabolic characterization of caco-2 cells expressing CYP3A4 and CYP3A4 plus oxidoreductase. *Pharm. Res.* **16**:1352–1359 (1999).
13. M. Kool, M. de Haas, G. L. Scheffer, R. J. Scheper, M. J. T. van Eijk, J. A. Juijn, F. Baas, and P. Borst. Analysis of expression of cMOAT(MRP2), MRP3, MRP4, and MRP5, homologues of the multi-drug resistance-associated protein gene (MRP1), in human cancer cell lines. *Cancer Res.* **57**:3537–3547 (1997).
14. J. M. Fisher, S. A. Wrighton, P. B. Watkins, P. Schmiedlin-Ren, J. C. Calamia, D. D. Shen, K. L. Kunze, and K. E. Thummel. First-pass midazolam metabolism catalyzed by 1α,25-dihydroxy vitamin D_3-modified caco-2 cell monolayers. *J. Pharmacol. Exp. Ther.* **289**:1134–1142 (1999).
15. J. Hunter, M. A. Jepson, T. Tsuruo, N. L. Simmons, and B. H. Hirst. Functional expression of p-glycoprotein in apical membranes of human intestinal caco-2 cells: Kinetics of vinblastine secretion and interaction with modulators. *J. Biol. Chem.* **268**: 14991–14997 (1993).
16. P. Anderle, E. Niederer, W. Rubas, C. Hilgendorf, H. Spahn-Langguth, H. Wunderli-Allenspach, H. P. Merkle, and P. Langguth. P-glycoprotein (p-gp) mediated efflux in caco-2 monolayers: The influence of culturing conditions and drug exposure on p-gp expression levels. *J. Pharm. Sci.* **87**:757–762 (1998).
17. R. Evers, G. J. R. Zaman, L. van Deemter, H. Jansen, J. Calafat, L. C. J. M. Oomen, R. P. J. Oude Elferink, P. Borst, and A. H. Schinkel. Basolateral localization and export activity of the human multidrug resistance-associated protein in polarized pig kidney cells. *J. Clin. Invest.* **97**:1211–1218 (1996).
18. R. Evers, M. Kool, L. van Deemter, H. Janssen, J. Calafat, L. C. J.M. Oomen, C. C. Paulusma, R. P. J. Oude Elferink, F. Baas, A.

H. Schinkel, and P. Borst. Drug export activity of the human canalicular multispecific organic anion transporter in polarized kidney MDCK cells expressing cMOAT (MRP2) cDNA. *J. Clin. Invest.* **101**:1310–1319 (1998).
19. P. B. Watkins, S. A. Wrighton, E. G. Schuetz, D. T. Molowa, and P. S. Guzelian. Identification of glucocorticoid-inducible cytochromes P-450 in the intestinal mucosa of rats and man. *J. Clin. Invest.* **80**:1029–1036 (1987).
20. L. Z. Benet, D. L. Kroetz, and L. B. Sheiner. Pharmacokinetics: The dynamics of drug absorption, distribution, and elimination. In J. G. Hardman, L. E. Limbird, P. B. Molinoff, R. W. Ruddon, and A. G. Gilman (eds.), *Goodman & Gilman's The Pharmacological Basis of Therapeutics*, McGraw-Hill, New York 1996 pp. 3–28.
21. K. Hosoya, K.-J. Kim, and V. H. L. Lee. Age-dependent expression of p-glycoprotein gp170 in caco-2 cell monolayers. *Pharm. Res.* **13**:885–890 (1996).
22. P. Artursson, A.-L. Ungell, and J.-E. Löfroth. Selective paracellular permeability in two models of intestinal absorption: Cultured monolayers of human intestinal epithelial cells and rat intestinal segments. *Pharm. Res.* **10**:1123–1129 (1993).
23. V. D. Makhey, A. Guo, D. A. Norris, P. Hu, J. Yan, and P. J. Sinko. Characterization of the regional intestinal kinetics of drug efflux in rat and human intestine and in caco-2 cells. *Pharm. Res.* **15**:1160–1167 (1998).
24. U. K. Walle, A. Galijatovic, and T. Walle. Transport of the flavonoid chrysin and its conjugated metabolites by the human intestinal cell line caco-2. *Biochem. Pharmacol.* **58**:431–438 (1999).
25. R. A. Walgren, K. J. Karnaky, Jr., G. E. Lindenmayer, and T. Walle. Efflux of dietary flavonoid quercetin 4′-β-glucoside across human intestinal caco-2 cell monolayers by apical multi-drug resistance-associated protein-2. *J. Pharmacol. Exp. Ther.* **294**:830–836 (2000).
26. G. L. Scheffer, M. Kool, M. Heijn, M. de Haas, A. C. L. M. Pijnenborg, J. Wijnholds, A. van Helvoort, M. C. de Jong, J. H. Hooijberg, C. A. A. M. Mol, M. van der Linden, J. M. L. de Vree, P. van der Valk, R. P. J. Oude Elferink, P. Borst, and R. J. Scheper. Specific detection of multidrug resistance proteins MRP1, MRP2, MRP3, MRP5, and MDR3 p-glycoprotein with a panel of monoclonal antibodies. *Cancer Res.* **60**:5269–5277 (2000).
27. M. J. Flens, G. J. R. Zaman, P. van der Valk, M. A. Izquierdo, A. B. Schroeijers, G. L. Scheffer, P. van der Groep, M. de Haas, C. J. L. M. Meijer, and R. J. Scheper. Tissue distribution of the multi-drug resistance protein. *Am. J. Pathol.* **148**:1237–1247 (1996).
28. M. J. Flens, M. A. Izquierdo, G. L. Scheffer, J. M. Fritz, C. L. M. Meijer, R. J. Scheper, and G. J. R. Zaman. Immunochemical detection of the multidrug resistance-associated protein MRP in human multidrug-resistant tumor cells by monoclonal antibodies. *Cancer Res.* **54**:4557–4563 (1994).
29. A. D. Mottino, T. Hoffman, L. Jennes, and M. Vore. Expression and localization of multidrug resistant protein mrp2 in rat small intestine. *J. Pharmacol. Exp. Ther.* **293**:717–723 (2000).
30. R. A. M. H. Van Aubel, A. Hartog, R. J. M. Bindels, C. H. Van Os, and F. G. M. Russel. Expression and immunolocalization of multidrug resistance protein 2 in rabbit small intestine. *Eur. J. Pharmacol.* **400**:195–198 (2000).